The Quantification of Risk Factors for Predicting Diabetic Cystoid Macular Edema based on a Hierarchical Approach

Eun Byeol Jo*, Ju Hwan Lee*, Jong Seob Jeong*, Byeong Cheol Choi† and Sung Min Kim*
*Department of Medical Biotechnology, Dongguk University-Seoul
Seoul, South Korea
{eunbyeol27, ykjhlee, jjsspace}@gmail.com, smkim@dongguk.edu
†Department of Biomedical Engineering, Choonhae College of Health Sciences
Ulsan, South Korea
bcchoi@ch.ac.kr

***Abstract*—This study suggests a novel risk factor extraction method for retina layers based on a hierarchical approach to distinguish Diabetic Cystoid Macular Edema (DCME) from optical coherence tomography scans. For this, a total of 80 subjects composed of 30 normal and 50 DCME patients were selected. To estimate evaluation variables, a hierarchical approach-based feature extraction algorithm was employed. Evaluation variables were classified into the Total Retina (TR), the Inner Retina (IR), the Photoreceptor Outer Segment (POS), the Outer Retina (OR), the Ganglion Cell (GC), and the Retinal Nerve Fiber Layer (RNFL). The experimental results show the reliable performance of the proposed approach in discriminating DCME from normal subjects. The proposed method could differentiate changes in the thickness of the IR and the POS between the normal and DCME groups. In addition, the most significant degeneration was observed in the central macular area. These results suggest the clinical applicability of the proposed method to the diagnosis of DCME.**

Keywords-diabetic cystoid macular edema; optical coherence tomography; retina layer; thickness; hierarchical approach

I. INTRODUCTION

Diabetic retinopathy is one of the most frequent complications caused by diabetes. The prevalence of diabetes has increased in an aging society, and patients with diabetic retinopathy have also been increasing. Among various types of diabetic retinopathy, Diabetic Cystoid Macular Edema (DCME) is a major cause of vision loss [1]. DCME increases the thickness of the retina by accumulating liquid inside through the collapse of the retinal barrier and causes macular degeneration at the center of the retina where images are focused on [2].

The diagnosis of DCME is usually performed using the Retinal Thickness Analyzer (RTA) [3], Heidelberg Retina Tomography (HRT) [4], and Optical Coherence Tomography (OCT) [5]. Among these techniques, OCT is known as the gold standard for diagnosing DCME [6] because of its superior sensitivity. OCT also allows for the quantitative measurement of retina lesions and structures. However, OCT cannot identify various intra-retinal structures accurately, and the accuracy of extracting macular thickness is relatively low. In particular, it represents the lowest accuracy for retina nerve fiber layers, where photoreceptors exist [7].

To address these problems, a number of studies have extracted macular thickness based on retinal layer boundaries from OCT images. Mujat et al. [8] proposed a novel boundary extraction approach for smoothing boundaries and reducing the image-processing speed based on the deformable spline algorithm. However, this method cannot process large amounts of data simultaneously. Koozekanani et al. [9] tried to minimize detection errors for retinal boundaries by using the standard Markov boundary model [10]. Bartsch et al. [11] simply extracted the longest boundary appearing continuously in the retina layer based on an improved Markov boundary model. Also, Yazdanpanah et al. [12] successfully segmented the retina and the choroid from OCT images by using a dual-thresholding technique and found the availability of only limited information. Gonzalez et al. [13] tried to identify retina layers by using the Hough transform, but this technique cannot successively extract various thickness values. Chiu et al. [14] extracted retinal layers by taking a graph-search segmentation approach using dynamic programming. Similarly, Yang et al. [15] minimized thickness measurement errors by applying the weight of graph-based dual-scale gradient information. The graph-search segmentation method used in the above two studies has a disadvantage in that it takes a long time to calculate because the number of operations varies widely according to the resolution of images.

This study estimates the risk factors of retina layers using a hierarchical approach-based feature extraction method to appropriately distinguish DCME from the original OCT scan. The rest of this paper is organized as follows: Section 2 develops the algorithm and discusses the background of the experiment. Section 3 presents the results, and Section 4 discusses them. Finally, Section 5 concludes.

II. MATERIAL AND METHODS

A. Image Acquisition

The experiment included a total of 80 subjects composed of 30 normal and 50 DCME patients. These subjects were classified into 50 normal and 100 DCME eyes based on a clinical evaluation with a trained operator. Retina images

 ISBN: 978-1-61208-367-4

were acquired using OCT (Cirrus HD-OCT, Carl Zeiss Meditec, Inc. Dublin, CA). The Institutional Review Board of Dongguk University Hospital approved this study, and all participants gave their consent to participate in the study.

B. Algorithm Development

To extract the thickness of retina layer, a modified hierarchical approach of Koprowski [16] was employed. First, denoised images were obtained by applying median filtering to the original OCT scan (Figure 1(b)). Then, the difference between the original image and the blurred image (image mask) was obtained, and synthesis outcomes for output and original images were printed. Images from the aforementioned step showed a low resolution. To measure the retina layer, the image was decomposed into pixels of *N x N* size *(N=15, 16, 17)* (Figure 1(c)). In addition, thresholding techniques using the Otsu algorithm were applied to separate the threshold in the degraded image (Figure 1(d)). The pixel value of the output image indicated the average value of the decomposed image into this *N x N* size. Based on the average value, the maximum pixel value in each column was derived as follows:

$$L_{DM}(m,n)=\begin{Bmatrix}1 & if & L_D(m,n)=\max_m(L_D(m,n))\\ 0 & other & \end{Bmatrix} \quad (1)$$

where *m* and *n* refer to rows and columns, respectively. Based on images acquired from (1), the top image boundary was obtained. The lowest boundary of the image was measured using the following (2):

$$L_{DM}(m,n)=\begin{Bmatrix}1 & if & |L_D(m,n)-L_D(m+1,n)|>P_r\\ 0 & other & \end{Bmatrix} \quad (2)$$

where P_r indicates the threshold in the (0, 0.2) range according to each pixel and satisfies $m \in (1, M-1)$, $n \in (1, N)$. Through this process, the bottom boundary of the retina layer was extracted, and upper and lower boundaries of the retina were obtained $(L_{DM}, L_{DB} = 1)$. The boundary coordinate showing a value of 1 in the output image was defined as $LDB\ (x) \leq LDM\ (x)$. The boundary coordinate was the output a total of three different boundary coordinate values based on pixel size. Figure 1(e) shows the synthesis results for the original image and three boundary outputs. This procedure was repeated to minimize errors during the detection of boundaries. The mean value of three boundary values was designated as the final boundary value (Figure 1(f)). All image processing was performed using the Matlab software (R2011b, MathWorks Inc., Natick, MA, USA).

C. Evaluation Variables

The proposed approach was employed to extract six risk factors, including the Total Retina (TR), the Inner Retina (IR), the Photoreceptor Outer Segment (POS), the Outer Retina (OR), the Ganglion Cell (GC), and the Retinal Nerve Fiber Layer (RNFL). The TR was the retina layer from the top boundary to the bottom edge (Figure 2), and the IR was the retina layer obtained by subtracting the OR and the POS

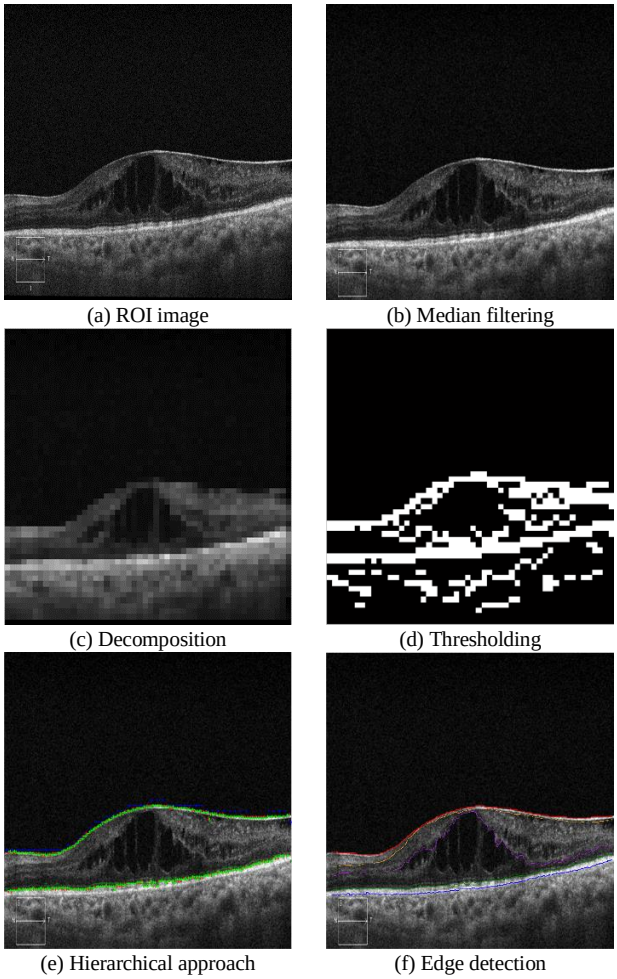

(a) ROI image (b) Median filtering (c) Decomposition (d) Thresholding (e) Hierarchical approach (f) Edge detection

Figure 1. Image processing procedures for obtaining the thickness of retina layer.

from the TR. The POS was the lowest retina layer, and the OR was the thickness of swelling in the retina layer. Cells were distributed in the GCL, which delivered visual information to the brain and was included in the TR. The

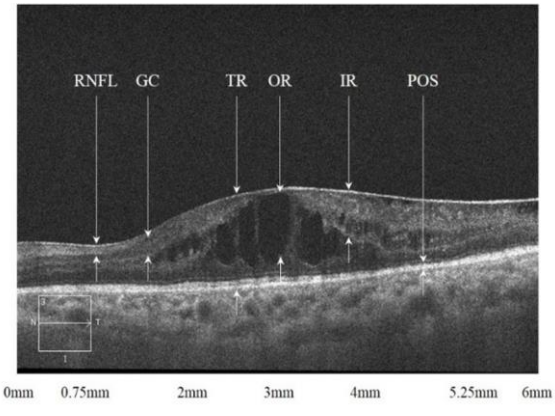

Figure 2. The specific positions of each evaluation variables in the OCT image.

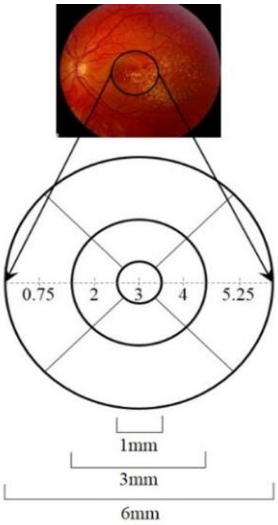

Figure 3. Regions for measuring risk factors from the center of the macula (0.75 mm, 2.00 mm, 3.00 mm, 4.00 mm, and 5.25 mm).

RNFL was the retina layer at the top and included optic nerve cells. Figure 2 shows the position of each evaluation variable in the OCT image.

Each evaluation variable was extracted from the original OCT image captured within a 3 mm radius from the center of the macula. OCT images were divided into a total of five measurements (0.75 mm, 2.00 mm, 3.00 mm, 4.00 mm, and 5.25 mm), and the average value of each measurement was specified as an evaluation variable (Figure 3).

D. Statistical Analysis

Data were analyzed using an independent t-test and a one-way ANOVA based on SPSS (Ver. 12.0 for Windows, Chicago, IL, USA). A p-value less than 0.05 was considered significant.

III. EXPERIMENTAL RESULTS

A. A Comparison of Thickness Extraction Performance between Cirrus HD-OCT and the Proposed Method

To evaluate the performance of the proposed extraction approach, evaluation variables were measured using Cirrus HD-OCT equipment, and statistical significance was compared. The OCT equipment was only able to measure the thicknesses of the TR, the GC, and the RNFL.

In the normal group, the proposed method showed higher reliability than the existing method. The R^2 value, which was used to evaluate the significance of variables, was close to 1 (Figure 4). On the other hand, the R^2 value of most evaluation parameters was close to 1 in the DCME group, but the RNFL showed a low value of 0.0446 (Figure 5(d)). TR and GC values extracted by Cirrus HD-OCT showed significant differences between the normal and DCME groups ($p < 0.05$). However, the RNFL showed a low level of significance ($p > 0.05$).

B. A Comparison of Retinal Layers between Normal and DCME Groups

According to correlations between evaluation variables for the normal and DCME groups, the TR, the OR, the GC, and the RNFL showed high levels of significance in all

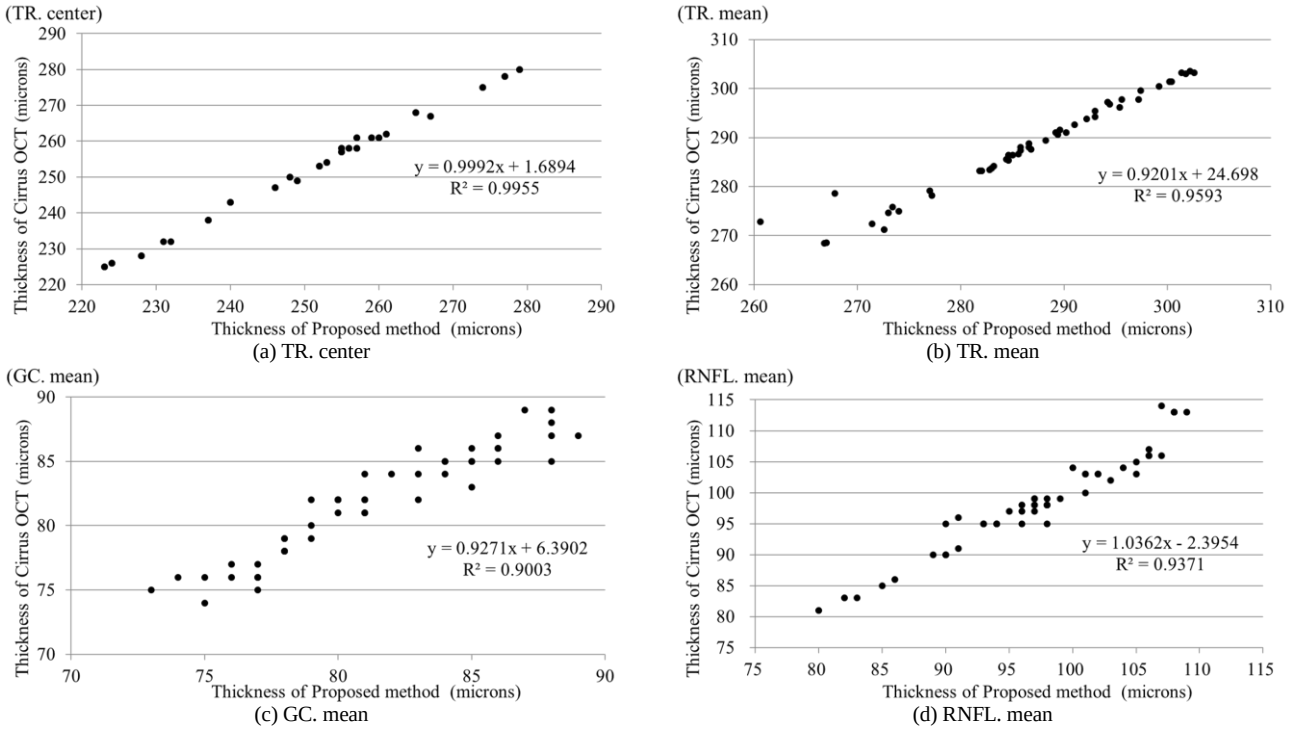

Figure 4. Comparison of the evaluation variables obtained from the Cirrus HD OCT and proposed method for normal subjects

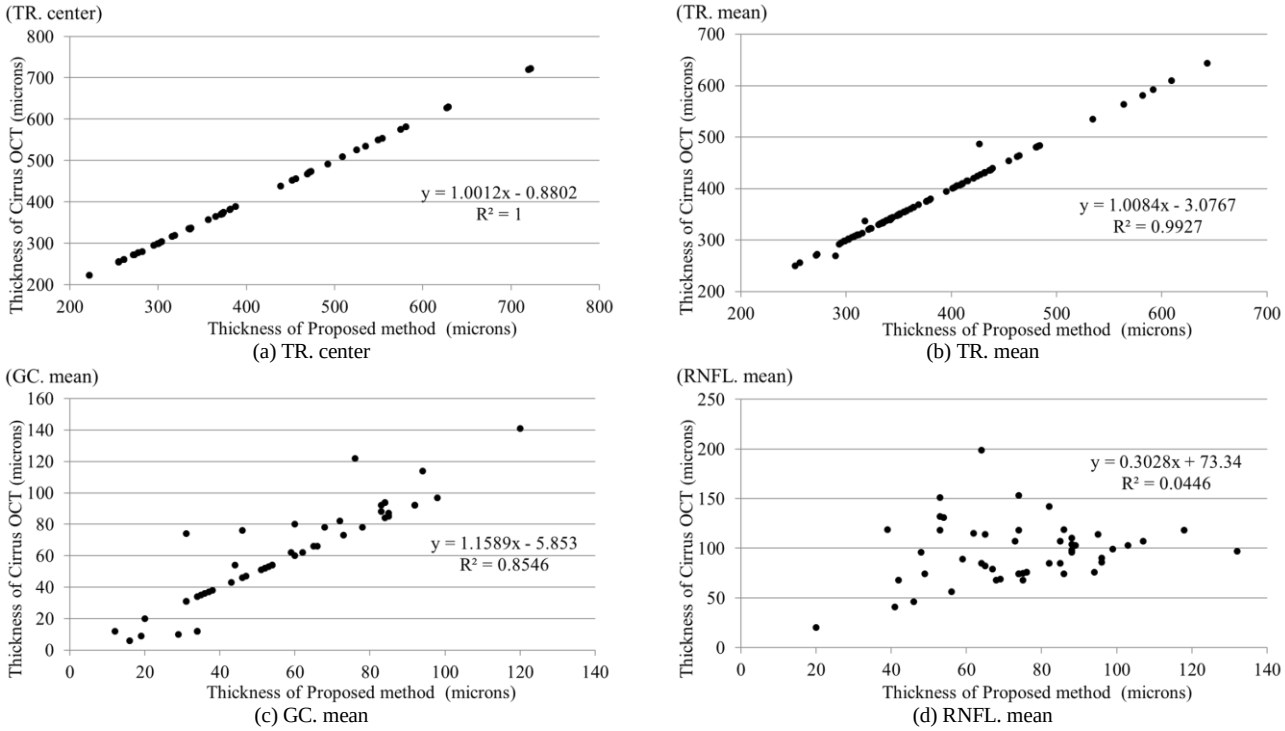

Figure 5. Comparison of the evaluation variables obtained from the Cirrus HD OCT and proposed method for DCME group

macular regions ($p < 0.05$). On the other hand, the IR and the POS showed high levels of significance in the normal and DCME groups only in the central macular region ($p < 0.05$), and the other areas showed a low level of significance.

The TR was thicker in the normal group than the DCME group in all macular regions. In particular, differences increased toward the center of the macula, and the largest difference (148.051 mm) was found at the center of the macular area. The IR was larger in the normal group than in the DCME group (except for the 4.5 mm - 6.0 mm range). The largest difference (78.494 mm) was found at the center of the macula. In addition, the POS was thicker in the normal group, and the difference at the center was 29.421 mm. Finally, the GC and the RNFL were larger in the normal group. The OR could be measured only in the DCME group. For all the aforementioned evaluation parameters, the standard deviation was higher in the DCME group than in the normal group. Table 1 compares evaluation parameters extracted using the proposed method between the normal and DCME groups.

IV. DISCUSSION

The proposed method could measure the thickness of the IR, the POS, and the OR, which could not be obtained using the existing method. It could also measure the TR, the GC, and the RNFL in OCT images. According to a comparison of experimental results based on Cirrus HD-OCT, extracted evaluation parameters were very similar to those based on the existing method. In addition, RNFL values obtained by Cirrus HD showed a low level of significance in discriminating between the normal and DCME groups, unlike in the case of other retina layers, providing no support for the suitability of clinical RNFL data for diagnosing DCME.

According to the statistical analysis of evaluation variables based on the proposed method between the normal and DCME groups, the TR, the GC, and the RNFL showed high levels of significance for the whole area of the macula. This indicates that extracted risk factors were significant predictors of DCME. On the other hand, the IR and the POS showed low levels of significance in some sections, and the center of the macula (clinically the most important area) showed a high level of significance in both normal and DCME groups. This implies the usefulness of the IR and the POS for diagnosing DCME.

According to a comparison of differences in evaluation variables between the normal and DCME groups, the TR was larger in the DCME group. This was mainly because the whole layer swelled up from retinal edema. The IR was much smaller in the DCME group than in the normal group. The decrease in the IR typically implies an increased risk of vision loss, since the IR includes the GC and the RNFL [17]. The POS tended to become thinner with retinal neovascularization, indicating greater damage. Given this, the POS was minutely thinner in the DCME group than in the normal group, indicating the worsening of retinal damage. In addition, the GC and the RNFL were larger in the normal group, indicating an increase in the risk of macular degeneration [18]. Further, the difference between the normal and DCME groups increased significantly in the macular area, the center of the retina, because abnormalities generally occur first in the macular area, where the optic

 ISBN: 978-1-61208-367-4

TABLE I. COMPARISON OF EVALUATION PARAMETERS EXTRACTED FROM OCT SCANS USING THE PROPOSED METHOD BETWEEN THE NORMAL AND DCME GROUPS

	Horizontal distance	Normal group	DCME group	P-value
TR	0~1.5mm	279.625±22.445	343.100±72.930	0.000
	1.5~2.5mm	318.333±13.760	398.520±94.999	0.000
	2.5~3.5mm	252.229±15.383	400.280±126.402	0.000
	3.5~4.5mm	314.917±17.140	394.470±92.306	0.000
	4.5~6mm	268.979±18.589	336.020±64.825	0.000
	Mean	286.817±11.245	374.478±76.799	0.000
IR	0~1.5mm	215.576±24.832	214.846±55.775	0.952
	1.5~2.5mm	251.106±34.584	215.614±63.400	0.004
	2.5~3.5mm	168.793±15.719	90.299±70.487	0.000
	3.5~4.5mm	252.800±14.517	227.090±51.097	0.003
	4.5~6mm	212.302±22.481	221.624±60.098	0.362
	Mean	220.117±12.231	193.893±34.351	0.000
POS	0~1.5mm	63.757±6.796	62.585±19.025	0.714
	1.5~2.5mm	67.102±30.696	56.722±15.494	0.069
	2.5~3.5mm	84.915±10.659	55.494±27.412	0.000
	3.5~4.5mm	63.825±6.575	57.990±15.890	0.380
	4.5~6mm	65.948±7.731	61.190±16.688	0.114
	Mean	69.108±5.854	58.796±10.447	0.000
OR	0~1.5mm	0.000±0.000	68.069±47.118	0.000
	1.5~2.5mm	-	130.505±95.987	0.000
	2.5~3.5mm	-	269.684±156.672	0.000
	3.5~4.5mm	-	130.807±105.306	0.000
	4.5~6mm	-	67.118±63.748	0.000
	Mean	-	133.237±70.990	0.000
GC	Minimum	77.667±4.984	30.640±24.854	0.000
	Mean	81.750±4.162	57.740±24.891	0.000
RNFL	Mean	95.708±8.143	73.900±21.461	0.000

nerve is mainly distributed. This implies that DCME may produce substantial degeneration in the central region of the macula and is closely related to blindness.

V. CONCLUSION

The results suggest that the proposed algorithm can reliably differentiate DCME patients from normal subjects. In addition, changes in the thickness of the IR and the POS may be useful risk factors for diagnosing DCME. Further, the most significant degeneration was observed in the central area of the macula as DCME progressed. These results suggest the clinical applicability of the proposed method to the diagnosis of DCME. This study has a limitation in that the normal and DCME groups had relatively small numbers of subjects. For more reliable results, future research should provide additional experiments using a larger number of test subjects and a wider range of classification models. In addition, the effects of age and gender should be considered in the context of DCME.

ACKNOWLEDGMENT

This work was supported by International Collaborative R&D Program funded by the Ministry of Knowledge Economy (MKE), Korea. (N01150049, Developing high frequency bandwidth [40-60 MHz] high resolution image system and probe technology for diagnosing cardiovascular lesion)

REFERENCES

[1] R. Klein, B. E. Klein, S. E. Moss, M. D. Davis, and D. L. DeMets, “The Wisconsin epidemiologic study of diabetic retinopathy. IV. Diabetic macular edema,” Ophthalmology, vol. 91, no. 12, Dec. 1984, pp. 1464-1474.

[2] B. E. Bouma, G. J. Tearney, and B. Bouma, “Handbook of optical coherence tomography,” Taylor & Francis, Marcel Dekker, Inc., New York, 2002.

[3] Y. Oshima, K. Emi, S. Yamanishi, and M. Motokura, “Quantitative assessment of macular thickness in normal subjects and patients with diabetic retinopathy by scanning

retinal thickness analyser," British Journal of Ophthalmology, vol. 83, no. 1, Jan. 1999, pp. 54-61.

[4] H. J. Zambarakji, W. M. Amoaku, and S. A. Vernon, "Volumetric analysis of early macular edema with the heidelberg retina tomograph in diabetic retinopathy," Ophthalmology, vol. 105, no. 6, Jun. 1998, pp. 1051-1059.

[5] M. R. Hee et al., "Quantitative assessment of macular edema with optical coherence tomography," Archieves of Ophthalmology, vol. 113, no. 8, Aug. 1995, pp. 1019-1029.

[6] D. F. Kiernan, W. F. Mieler, and S. M. Hariprasad, "Spectral-domain optical coherence tomography: a comparison of modern high-resolution retinal imaging systems," American Journal of Ophthalmology, vol. 149, no. 1, Jan. 2010, pp. 18-31.

[7] F. A. Medeiros et al., "Evaluation of retinal nerve fiber layer, optic nerve head, and macular thickness measurements for glaucoma detection using optical coherence tomography," American Journal of Ophthalmology, vol. 139, no. 1, Jan. 2005, pp. 44-55.

[8] M. Mujat et al., "Retinal nerve fiber layer thickness map determined from optical coherence tomography images," Optics Express, vol. 13, no. 23, Nov. 2005, pp. 9480-9491.

[9] D. Koozekanani, K. Boyer, and C. Roberts, "Retinal thickness measurements from optical coherence tomography using a Markov boundary model," IEEE Transactions on Medical Imaging, vol. 20, no. 9, Sep. 2001, pp. 900-916.

[10] P. Zhou and D. Pycock, "Robust statistical models for cell image interpretation," Image and Vision Computing, vol. 15, no. 4, Apr. 1997, pp. 307-316.

[11] D. U. G. Bartsch, X. Gong, C. Ly, and W. R. Freeman, "Optical coherence tomography: interpretation artifacts and new algorithm," Proc. SPIE 5370, Medical Imaging 2004: Image Processing, May 2004, pp. 2140-2151.

[12] A. Yazdanpanah, G. Hamarneh, B. Smith, and M. Sarunic, "Intra-retinal layer segmentation in optical coherence tomography using an active contour approach," Lecture Notes in Computer Science, vol. 5762, Sep. 2009, pp. 649-656.

[13] R. C. Gonzalez and R. E. Woods, "Digital image processing (3rd edition)," Prentice Hall, 2008.

[14] S. J. Chiu et al., "Automatic segmentation of seven retinal layers in SDOCT images congruent with expert manual segmentation," Optics Express, vol. 18, no. 18, Aug. 2010, pp. 19413-19428.

[15] Q. Yang et al., "Automated layer segmentation of macular OCT images using dual-scale gradient information," Optics Express, vol. 18, no. 20, Sep. 2010, pp. 21293-21307.

[16] R. Koprowski and Z. Wróbel, "Image processing in optical coherence tomography," Katowice, Poland, 2011.

[17] H. Ishikawa et al., "Macular segmentation with optical coherence tomography," Investigative Ophthalmology & Visual Science, vol. 46, no. 6, Jun. 2005, pp. 2012-2017.

[18] J. C. Brown et al., "Detection of diabetic foveal edema: contact lens biomicroscopy compared with optical coherence tomography," Archieves of Ophthalmology, vol. 122, no. 3, Mar. 2004, pp. 330-335.

 ISBN: 978-1-61208-367-4